Evaluation of Multiphase Flow Rate Models for Chokes Under Subcritical Oil/Gas/Water Flow Conditions

R.B. Schüller, Agricultural U. of Norway; **T. Solbakken,** SPE, Norsk-Hydro ASA; and **S. Selmer-Olsen,** Det Norske Veritas AS

Summary

Knowing the mass flow rate is important in relation to production control in the oil and gas industry. If the change in pressure and temperature across a choke can be correlated with the mass flow rate, the actuator position, and the properties of the well stream, this may constitute a mass flow rate meter that is both simple and inexpensive compared to other designs. However, knowledge of the predictive ability and accuracy of available mass flow rate models is required to qualify such a solution. Predictions from several mass flow rate models are compared with data from a crude oil/natural gas/water system at pressures varying from 8 to 16 bara. The fluids used were recombined oil from the Njord field in the North Sea, natural gas from the Kaarstoe terminal in Norway, and water with added salts to give typical produced-water properties. Two different choke geometries (orifice and cage type) were tested for three different opening areas. The experimental results are compared with eight mass flow rate models for multiphase flow through chokes. These are the two Hydro models originally developed by Selmer-Olsen, the Sachdeva *et al.* model, the Perkins' model, and four two-phase multiplier models—the Morris, the Chisholm, the Simpson, and the homogeneous equilibrium model (HEM), respectively. For the orifice-type geometry, the Hydro short model predicted the results most accurately. For the cage-type geometry, the Hydro long model, which includes losses in the choke geometry, predicted the results most accurately. A modification to the slip model improves the results of the Hydro models, predicting all the 367 test points with a standard deviation of 7.8%. The average error of absolute values was 5.8%.

Introduction

The flow of multiphase flow systems is important in the process industry in relation to both the control of process conditions and to safety in relation to the overpressure control by relief valves. In the oil and gas industry, the flow characteristics of the choke control the production of oil/gas/water coming from the wells. For reservoirs with advanced well systems, including more than one flow branch tied back to a common manifold, it is essential to control the individual well streams by individual chokes. Managing this production control becomes even more critical when producing from horizontal wells and thin oil zones.

In recent years, tools for well allocation and control have been developed with the intention of determining the mass flow rate from a minimum of data about the multiphase conditions in the upstream tubing, the fluid properties, and the choke characteristics. Such choke characteristics range through both subcritical and critical flow conditions. These tools use both traditional flow models from the literature as well as new models developed specifically for choke control in the hydrocarbon production industry.

The objective of the present work was to develop a unique data set for validation of such flow models and to use it in a benchmarking exercise to evaluate the suitability of some typical models in use. The present paper focuses on the subcritical part of the data set obtained under controlled laboratory conditions with hydrocarbons from North Sea oil fields.

The main difference between hydrocarbon well streams and single-component systems are that well fluids include a large number of components, from light to heavy hydrocarbons. The kinetics caused by flashing of the light components through a choke are expected to be different than single-component systems. Furthermore, reservoir fluids often include a separate water phase in addition to the gas and oil phases.

Depending on the upstream geometry and flow rates, several different flow patterns exist that will influence the choke conditions (such as liquid slugs, phase inversion phenomena, etc.). Moreover, the choke geometry influences choke flow patterns.

Literature

The literature survey focused on fairly simple models that provide a relationship between the multiphase mass flow rate, $\dot{m}$, the choke pressure drop, Δp, the model parameters, data for upstream and downstream pressure and temperature, upstream composition of the well stream (oil, water, and gas), and the choke setting (opening). Model imperfections or simplifications would typically be corrected by introducing a calibration factor.

Choke manufacturers have ways of sizing and selecting wellhead chokes normally based on a flow coefficient C_V often determined in a test bench with water flow.[1] The flow coefficient for valve sizing, C_V, has, by definition, the dimension of the flow rate of water in gal/min for a pressure drop of 1 psi.[2] Using SI units for the right side, we obtain the following expression for C_V.

$$C_V = \frac{3600}{0.86}\frac{\dot{Q}}{F_\gamma}\sqrt{\frac{\rho_m}{\rho_W}\frac{10^5}{\Delta p}}\,\Delta p = p_1 - p_3. \quad \ldots\ldots\ldots\ldots\ldots\ldots (1)$$

in which $\dot{Q}$ = volumetric flow rate, ρ = density, F_γ = choked flow factor, and Δp = pressure difference. The subscripts m and W denote multiphase mixture and water, respectively. The subscripts 1 and 3 denote inlet and outlet positions, respectively. $F_\gamma = 1$ for subcritical flow. If Eq. 1 is used for single-phase water flow, use $\rho_m = \rho_w$. Normally, the homogeneous mixture density, ρ_m, is used, which can be found with Eq. 15.

Several mass flow rate models are based on the classical single-phase approach. The basic idea is to correct for the impact of two-phase flow on the pressure drop by introducing a correction factor—two-phase multiplier.[3] The two-phase multiplier, Φ, is the ratio between the actual two-phase pressure drop and the single-phase liquid pressure drop, subscript LO, with similar two-phase and single-phase mass flow rates. Compressible flow is not accounted for. The expression is given as:

$$\Phi_{LO}^2 = \frac{\Delta p}{\Delta p_{LO}}. \quad \ldots\ldots\ldots\ldots\ldots\ldots\ldots\ldots\ldots\ldots\ldots\ldots\ldots\ldots (2)$$

Recasting Eq. 1 to the form of Eq. 2 shows that the approach is the same.

To account for compressibility effects and critical flow in multiphase flow, several approaches are found, such as:

- Homogeneous flow models assuming no flashing of gas from the oil through the choke ("frozen" flow).[4]
- Homogeneous flow models[5,6] that assume thermodynamic equilibrium.

This paper (SPE 84961) was revised for publication from paper SPE 72088. Original manuscript received for review 18 April 2001. Revised manuscript received 25 March 2003. Paper peer approved 30 April 2003.

• Models assuming empirical or semi-empirical relations describing the kinetics of flashing of gas from the liquid and/or entrainment of one phase in the other based on single-component steam-water systems.[7]

• Heterogeneous flow models of a gas and a liquid phase flowing separately and without one phase being entrained in the other.[5,8]

Most of these models can also be used for subcritical flow with minor modifications, but this is seldom done.

Sachdeva *et al.*[9] presented a model developed to solve the mass flow rate through a choke for both subcritical and critical conditions. This model has also been verified against multiphase experiments. The model assumes the flow is 1D, the phase velocities are equal at the throat, the predominant pressure term is acceleration, the quality is constant for high-speed processes, and the liquid phase is incompressible.

Robertson[1] observed up to 30% discrepancies between the manufacturer's published values for C_V and those determined for nonflashing flows of water/nitrogen and kerosene/methane. With flashing flows, the discrepancies were even larger. They found no better results with other methods from the literature, so they curve-fit correlations for an improved flow coefficient, C_V. BP plc presented an improved version of these models.[10]

The Perkins models[11] presented an approach for finding the critical pressure ratio and the mass flow rate in much the same way as the model by Sachdeva *et al.* Perkins included the three-phase effects for the polytropic expansion exponent, n, and also found the mixture average velocity at the throat. The model solves the conservation equations for total energy and mass and applies a classical thermodynamics approach for the gas properties, which leads to an implicit expression to find the critical pressure ratio.

Osman and Dokla[12] presented a literature overview of choke models and a set of new empirical correlations for upstream pressure or choke pressure drop vs. choke size, flow rate, and gas/liquid ratio (GLR). They used field data for surface chokes of a Middle East gas-condensate reservoir.

Selmer-Olsen developed a set of new choke models[13,14] based on their own works.[15] The model versions and software in use originate from projects for Norsk Hydro ASA that studied the feasibility of using wellhead chokes as simple multiphase flow meters for production control of oil and gas. These models, now referred to as the Hydro models, use a control volume approach and cover both subcritical and critical conditions.

Test Facility and Methods

The experiments were performed in the multiphase flow loop (MPFL) (see **Fig. 1**) of Norsk Hydro ASA, located in Porsgrunn, Norway. The MPFL is a recirculating test facility for hydrocarbon/water mixtures built with complete control of system chemistry so that tests can be performed with the addition of production chemicals at ppm levels. The MPFL has a total volume of approximately 9 m^3, including a 77.9-mm internal diameter (ID) test loop that is 120 m long.

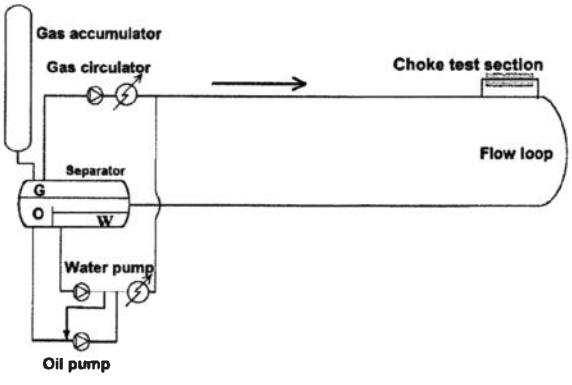

Fig. 1—The MPFL.

A test section designed geometrically as a choke was installed at the middle of the test loop, as shown in **Figs. 1 and 2.** The test conditions chosen had a downstream separator pressure of 8 bara. The gas circulator could operate at this condition with a maximum 8-bar pressure rise, giving a maximum choke upstream pressure of 16 bara. The accuracy of the pressure transmitters was better than 0.1% of full-scale reading.

Two different choke geometries were tested—an orifice and a simplified cage-type with two opposing holes. They were both designed and installed with the same reference position in the pipe. Both geometries were tested at three different flow areas. Because the cage-type geometry had two holes, these holes were sized to give the same total flow area compared to the equivalent orifice-type choke. The orientation of the holes was in the same horizontal plane.

Orifice and cage geometry represent two different flow behaviors for an obstruction in a pipe. The pressure over an orifice choke will reach a minimum immediately after the obstruction, whereas for a cage choke, the minimum pressure will be inside the obstruction. For cage chokes, a radial inflow through the cage causes flow impingement of two opposing jets in the cage center. In the cage geometry, this turbulent impingement creates pressure losses through internal dissipation, whereas for orifice geometry, the turbulent flow separation after the orifice creates pressure losses. The choke geometries are shown in **Fig. 3.** The three orifice diameters tested were 11, 14, and 18 mm, which represent 2.0, 3.5, and 5% choke opening areas, respectively, in a 77.9-mm ID tubing.

The test program included single-phase tests with gas, water, and oil. Further, two-phase gas/water and gas/oil tests were carried out, and three-phase gas/oil/water tests were performed last.

The fluids used were recombined oil from the Njord field in the North Sea, natural gas from the Kaarstoe terminal in Norway, and fresh water with added salts to give typical produced-water properties. The composition of the gas and the oil phase at 10 bara and 50°C are shown in **Table 1.** All components heavier than Pentane are denoted C6+.

The separator conditions were kept constant at 8 bara and 50°C during all tests. The independent test variables were the volumetric flow rates of each phase at separator conditions, and the response was the pressure difference and temperature over the choke. Hence, the upstream choke pressure varied from one test to another, whereas the downstream choke pressure was close to the constant separator pressure.

The densities of gas, oil, and water were known from the location where the volumetric flow rates were measured. The mass flow rate was constant during each test. The mass fractions of each phase, however, changed as the pressure decreased from the upstream choke condition to the separator condition because more gas dissolves at the higher pressure in the oil phase and because some liquid flashed.

The oil/gas/water stream was in equilibrium at a condition of GLR and water cut (WC) corresponding to the inlet of the separator. The upstream choke pressure was higher than the separator pressure, resulting in a different GLR and WC at the choke inlet. The values upstream of the choke were calculated with the thermodynamic property program NEW*S[16,17] based on thermodynamic equilibrium using the SRK equation of state. Because the temperature was constant, a pressure increase would normally cause more gas to be dissolved in the oil phase.

Experimental Results

A total of 367 tests were performed on six different test-section geometries. A selection of the complete results for one of these geometries, the 11-mm orifice, is included in **Table 2.** However, results from all 367 tests are included in the model comparisons presented in this paper.

Table 3 shows the C_V values for two different chokes and for three different opening areas. These values were obtained for single-phase water flow with Eq. 1 and then used as input to the two-phase multiplier models Eq. 2. The values are based on linear regression curves for all the multiphase-water data points for the

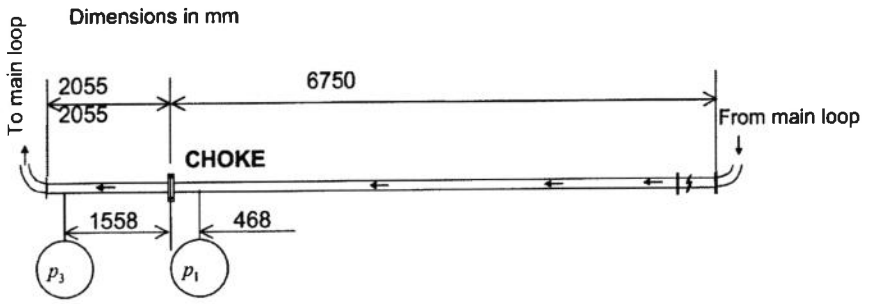

Fig. 2—Details of test section showing the positions of the choke and pressure tappings.

specific choke setting. Values of the regression coefficient, r^2, are also given in Table 3.

Models

Several mass flow models were tested against the experimental results from the MPFL. These were the Hydro models,[14] the models of Sachdeva *et al.*[9] and Perkins,[11] and four two-phase multiplier models.[3,18,19] Note that the Hydro model may be regarded as several models, as described in Ref. 14. Different slip assumptions were evaluated for this model. Only one of the possible assumptions regarding thermodynamic equilibrium was tested.

The Hydro, Sachdeva *et al.*, and Perkins models are all in use concurrently by the petroleum industry to control multiphase flow through chokes. The two-phase multiplier models were chosen merely as references. Because the Sachdeva *et al.* and Perkins models are accessible in SPE publications, the Hydro models are described in more detail here.[9,11]

Two-Phase Multiplier Models. Homogeneous equilibrium model (HEM):

$$\Phi_{LO}^2 = 1 + x_G\left[\frac{v_G}{v_L} - 1\right], \quad \ldots\ldots\ldots\ldots\ldots\ldots\ldots\ldots\ldots\ldots (3)$$

in which x = mass fraction and v = specific volume. The subscripts G and L denote gas and liquid, respectively.

Simpson *et al.*[19]:

$$\Phi_{LO}^2 = \left[x_G\frac{v_G}{v_L} + k(1-x_G)\right]\left[x_G + \frac{(1-x_G)}{k}\right]k = \left[\frac{v_G}{v_L}\right]^{1/6}, \quad \ldots (4)$$

here k = the slip correlation (see also **Table 4**).

$$\text{Chisholm}^3\text{: } \Phi_{LO}^2 = 1 + \left(\frac{v_G}{v_L} - 1\right)[Bx_G(1-x_G) + x_G^2]. \quad \ldots\ldots (5)$$

The coefficient B is determined by choke geometry and installation. $B = 0.5$ was chosen for our setup.

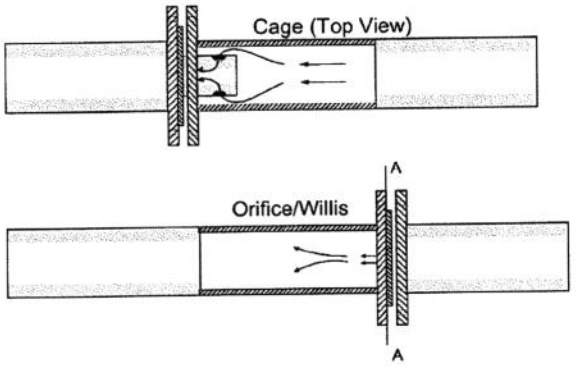

Fig. 3—Choke geometries.

Morris[18]:

$$\Phi_{LO}^2 = \left[x_G\frac{v_G}{v_L} + k(1-x_G)\right]\left[x_G + \frac{(1-x_G)}{k}\left(1 + \frac{(k-1)^2}{\sqrt{\frac{v_G}{v_L}}}\right)\right], \quad \ldots\ldots\ldots\ldots\ldots\ldots (6)$$

in which Morris used the slip correlation of Chisholm for k.

$$k = \left[x_G\frac{v_G}{v_L} + (1-x_G)\right]^{1/2}. \quad \ldots\ldots\ldots\ldots\ldots\ldots (7)$$

The single-phase water tests were used as input into the two-phase multiplier models. Note that neither two-phase multiplier model accounts for compressibility effects because upstream conditions were used as data to calculate the multiplier value.

Sachdeva *et al.* Model. The model of Sachdeva *et al.*[9] is developed from the 1D balance equations of mass, momentum, and energy for a two-phase mixture of gas and liquid. The gas quality is constant (frozen flow), and the liquid is incompressible. The phase velocities move homogeneously, whereas the phase temperatures could differ with the heat transfer process controlled by a polytropic expansion of the gas. The flow is adiabatic and frictionless. The model can handle both subcritical and critical flow. The model uses a discharge coefficient C_D in the range 0.75 to 0.85 to calibrate for model imperfections and irreversible losses.

Perkins Model. The Perkins model[11] is developed from the 1D balance equations of mass and energy. Contrary to the Sachdeva *et al.* model, Perkins uses the gas-phase energy equation instead of the mixture momentum equation. As for the Sachdeva *et al.* model, the phase velocities move homogeneously, whereas the gas phase is assumed to expand polytropically. The flow is adiabatic and frictionless, and the model can handle both subcritical and critical flow. Perkins found the best fit between prediction and experimental data by giving the discharge coefficient the value $C_D = 0.826$ to calibrate for model imperfections and irreversible losses.

Hydro Long Model. Contrary to the models of Sachdeva *et al.*[9] and Perkins,[11] this model[14] uses a control-volume approach for the choke orifice and downstream. This features a more mechanistic description of the irreversible loss process than a discharge coefficient only. If needed, a final fine-tuning could be done with a discharge or calibration coefficient. A control-volume approach also features a simple approach to a complex flow with heat and mass transfer phenomena. The approach assumes no loss of stagnation pressure and mixture enthalpy (temperature) up to the flow throat (*vena contracta**), and this gives the inlet conditions to the downstream control volume part of the model. The flow path may change direction before it enters the control volume but not within them.

The model is derived from the local cross-sectional averaged balance equations for steady-state flow of a multiphase mixture.

* Where the boundary streamlines form a minimum cross section.

TABLE 1—MOLAR COMPOSITIONS, VISCOSITY, AND DENSITY AT 10 BARA AND 50°C			
	Gas Phase	Oil Phase	Water Phase
Nitrogen	0.0156	0.0002	0.0000
Carbon dioxide	0.0079	0.0006	0.0000
Methane	0.8304	0.0333	0.0001
Ethane	0.0763	0.0147	0.0000
Propane	0.0238	0.0140	0.0000
Iso-butane	0.0052	0.0066	0.0000
Butane	0.0141	0.0254	0.0000
Iso-pentane	0.0041	0.0163	0.0000
Pentane	0.0048	0.0251	0.0000
C6+	0.0044	0.8624	0.0000
Water	0.0134	0.0014	0.9999
TOTAL	1.0000	1.0000	1.0000
Viscosity (mPas)	0.012	1.31	0.55
Density (kg/m^3)	7.7	796	988

$$\text{Mass balance: } \frac{d}{dz}(\dot{m}) = 0, \quad \ldots\ldots\ldots\ldots\ldots\ldots\ldots\ldots (8)$$

in which $\dot{m}$ = the mass flow rate of the multiphase mixture and z = the axial coordinate.

$$\text{Momentum: } \frac{d}{dz}\left(\frac{\dot{m}^2}{\rho_e A}\right) + A\frac{dp}{dz} = -\phi_w \tau_w - A\,\rho_m g \sin\theta, \quad \ldots. (9)$$

in which p = pressure, g = gravitational acceleration, A = the area of a flow cross section, ϕ_w = the wall perimeter, τ_w = wall shear stress, ρ_m = mixture density, ρ_e = momentum density, and θ = the angle of the flow path with the horizontal. The mechanical energy balance is obtained by integrating the momentum balance and the mass balance from conditions at Points 1 to 2 in **Fig. 4.**

$$\frac{\dot{m}^2}{2}\left(\frac{1}{\rho_{e2}^2 A_2^2} - \frac{1}{\rho_{e1}^2 A_1^2}\right) + \int_1^2 \frac{1}{\rho_e} dp + \int_1^2 \frac{\rho_m}{\rho_e} g \sin\theta dz = \Phi, \quad \ldots.. (10)$$

where Φ = irreversible losses from friction or internal viscous dissipation (the rate mechanical energy is converted to thermal energy). In a reversible flow, $\Phi = 0$.

$$\text{Total energy: } \frac{d}{dz}\left(h_m + \frac{\dot{m}^2}{2\rho_k^2 A^2} + \frac{\rho_m}{\rho_k} g \sin\theta z\right) = q_w, \quad \ldots\ldots. (11)$$

where h_m = mixture enthalpy, ρ_k = kinetic energy density, and q_w = heat flux through wall.

Mixture enthalpy, h_m, is found by weighing the enthalpies of each component or phase with their mass or mole fraction.

A distinction between different densities is required because the contribution of each phase will be weighed differently depending on whether the density is based on the mass in a control volume (body or potential force), giving ρ_m; the net momentum flow through a control volume (surface force), giving ρ_e; or the net kinetic energy flow through a control volume, giving ρ_k. The derivation of the density expressions is fairly straightforward algebra. The definitions are consistent with Chisholm.[3] The mixture density, ρ_m (specific volume v_m), is as follows.

$$v_m = \frac{1}{\rho_m} = \frac{1}{\alpha\rho_G + (1-\alpha)\rho_L} = \frac{\frac{x_G}{\rho_G} + k\frac{(1-x_G)}{\rho_L}}{x_G + k(1-x_G)}, \quad \ldots\ldots\ldots. (12)$$

where α = void fraction, x_G = gas quality, k = slip factor between gas and liquid phase, ρ_G = gas density, and ρ_L = density of liquid phase (oil and water mixture). The effective momentum density, ρ_e (specific volume v_e), is as follows.

$$v_e = \frac{1}{\rho_e} = \left[\frac{x_G}{\rho_G} + k\frac{(1-x_G)}{\rho_L}\right]\left[x_G + \frac{(1-x_G)}{k}\right]. \quad \ldots\ldots\ldots. (13)$$

The kinetic energy density, ρ_k (specific volume v_k), is:

$$v_k = \frac{1}{\rho_k} = \left[\frac{x_G}{\rho_G} + k\frac{(1-x_G)}{\rho_L}\right]\sqrt{x_G\frac{(1-x_G)}{k^2}}. \quad \ldots\ldots\ldots. (14)$$

The homogeneous mixture density, ρ_H (specific volume v_H), is found from Eqs. 12, 13, or 14 for $k = 1$.

$$v_H = \frac{1}{\rho_H} = \frac{x_G}{\rho_G} + \frac{(1-x_G)}{\rho_L}. \quad \ldots\ldots\ldots\ldots\ldots\ldots\ldots (15)$$

For liquid density, ρ_L = the homogeneous liquid mixture of oil and water used.

$$\rho_L = W_C\rho_w + (1 - W_C)\rho_O, \quad \ldots\ldots\ldots\ldots\ldots\ldots\ldots (16)$$

where ρ_w = water density, ρ_o = oil density, and W_C = water cut.

The model is based on the circular-symmetric flow geometry shown in Fig. 4. The flow separates at Position 2, the abrupt enlargement after the throat. The choke outlet at Position 3 is located after the flow reattachment point. The distances between Positions 1, V, 2, and 3 are chosen arbitrarily. The mixture balance equations for mass, momentum, and total energy are applied, assuming steady-state flow and neglecting gravity.

Upstream of V, there is no loss of stagnation pressure or change in mixture enthalpy. Downstream of V, there are two control volumes. The first is the dotted box starting at V, and the second is the dotted box starting at 2. Loss of stagnation pressure is allowed for in both control volumes. In the throat, internal dissipation and wall friction dominate, whereas downstream of Position 2, flow separation and shock waves dominate. After flow reattachment, wall friction and heat transfer effects can be present. Position 3 is chosen such that internal dissipation losses dominate, and the flow is frictionless and adiabatic from Position 2 to 3. In Position 3, the flow has homogeneous phase velocities, whereas velocity slip is allowed between Positions 1 and 3.

The flow is adiabatic between Positions 1 and 3, but it is assumed that the flow pattern is sufficiently dispersed to neglect temperature differences between the gas and the liquid. The flow is assumed to be frozen (constant vapor quality) upstream of Position 2. All phase changes occur in the control volume between Positions 2 and 3 such that thermal equilibrium is reassumed at Position 3. This is justified by observing that if flow components flash on the passage from Position 1 to 3, this process is associated with a certain time delay. Moreover, typical compositions from the North Sea will have flash fractions of only a few mass percent. The mixture density is regarded as constant between V and 2. In case the flow chokes, the critical section (C) is at Position 2.

From cross section 1 to 2, the mass and mechanical energy balances give:

$$\int_1^2 \frac{\rho_{e1}}{\rho_e} dp = \frac{\dot{m}^2}{2A_1^2\rho_{e1}}\left[\begin{array}{l} 1 - \left(\frac{\rho_{e1}}{\rho_{e2}}\right)^2 \frac{1}{C_T^2 C_C^2} \\ +2\left(\frac{\rho_{e1}}{\rho_{e2}}\right)^2 \frac{1}{C_T^2}\left(\frac{1}{C_C} - 1\right) \end{array}\right], \quad \ldots\ldots\ldots (17)$$

TABLE 2—RESULTS FOR THE 11-MM DIAMETER ORIFICE GEOMETRY

Test Point	p_1 (bara)	T_1 (°C)	x_{G1}	x_{O1}	x_{W1}	$p_1 - p_3$ (bar)	$\dot{m}$ (kg/s)
G-OR-11-01	8.47	52.9	1.0000	0.0000	0.0000	0.85	0.05
G-OR-11-02	10.00	51.9	1.0000	0.0000	0.0000	2.43	0.09
G-OR-11-03	12.20	52.9	1.0000	0.0000	0.0000	4.68	0.13
G-OR-11-04	13.90	51.9	1.0000	0.0000	0.0000	6.56	0.16
O-OR-11-01	8.37	49.9	0.0000	1.0000	0.0000	0.74	0.57
O-OR-11-02	9.18	49.9	0.0000	1.0000	0.0000	1.64	0.90
O-OR-11-03	10.60	50.9	0.0000	1.0000	0.0000	3.17	1.27
O-OR-11-04	12.50	49.9	0.0000	1.0000	0.0000	5.07	1.65
O-OR-11-05	14.90	50.9	0.0000	1.0000	0.0000	7.59	2.01
W-OR-11-01	8.36	49.9	0.0000	0.0000	1.0000	0.85	0.77
W-OR-11-02	9.74	50.9	0.0000	0.0000	1.0000	2.27	1.29
W-OR-11-03	12.40	50.9	0.0000	0.0000	1.0000	4.88	1.91
W-OR-11-04	15.80	50.9	0.0000	0.0000	1.0000	8.42	2.30
GOW-OR-11-01	8.41	50.9	0.0083	0.8620	0.1300	0.98	0.66
GOW-OR-11-02	9.50	49.9	0.0105	0.8780	0.1110	2.01	0.95
GOW-OR-11-03	11.40	49.9	0.0086	0.8630	0.1280	3.83	1.36
GOW-OR-11-04	13.10	50.9	0.0039	0.8790	0.1170	5.60	1.65
GOW-OR-11-05	14.00	50.9	0.0048	0.8600	0.1350	6.57	1.86
GOW-OR-11-06	8.74	49.9	0.0127	0.4330	0.5540	1.05	0.66
GOW-OR-11-07	10.10	49.9	0.0111	0.4490	0.5400	2.60	1.08
GOW-OR-11-08	11.50	50.9	0.0041	0.4540	0.5420	4.05	1.49
GOW-OR-11-09	13.80	50.9	0.0048	0.4490	0.5460	6.31	1.87
GOW-OR-11-10	8.87	50.9	0.0097	0.0916	0.8990	1.03	0.71
GOW-OR-11-11	9.84	52.9	0.0078	0.0709	0.9210	2.44	1.12
GOW-OR-11-12	11.70	52.9	0.0040	0.0896	0.9060	4.31	1.59
GOW-OR-11-13	13.80	49.9	0.0042	0.0786	0.9170	6.44	1.99
GOW-OR-11-14	10.80	50.9	0.0879	0.7810	0.1310	3.27	0.64
GOW-OR-11-15	12.00	49.9	0.0455	0.8470	0.1080	4.41	1.03
GOW-OR-11-16	14.00	50.9	0.0361	0.8740	0.1260	6.28	1.37
GOW-OR-11-17	14.80	51.9	0.0274	0.8570	0.1160	7.27	1.62
GOW-OR-11-18	10.60	50.9	0.0802	0.3770	0.5420	3.11	0.67
GOW-OR-11-19	12.10	50.9	0.0440	0.4180	0.5380	4.57	1.09
GOW-OR-11-20	14.40	49.9	0.0334	0.4340	0.5330	6.79	1.51
GOW-OR-11-21	15.50	50.9	0.0217	0.4430	0.5360	7.97	1.81
GOW-OR-11-22	11.60	50.9	0.0825	0.0575	0.8600	3.87	0.75
GOW-OR-11-23	14.40	50.9	0.0585	0.0968	0.8450	6.74	1.21
GOW-OR-11-24	14.80	50.9	0.0347	0.0407	0.9250	7.21	1.55
GOW-OR-11-25	12.50	50.9	0.1380	0.7290	0.1340	5.16	0.63
GOW-OR-11-26	14.20	50.9	0.0845	0.8030	0.1130	6.84	1.01
GOW-OR-11-27	13.40	50.9	0.1340	0.3730	0.4930	6.08	0.74
GOW-OR-11-28	14.30	50.9	0.0716	0.4160	0.5130	6.88	1.13
GOW-OR-11-29	14.10	50.9	0.1190	0.0957	0.7850	6.48	0.82
GOW-OR-11-30	14.70	50.9	0.0621	0.1090	0.8290	7.36	1.24
GOW-OR-11-31	14.20	50.9	0.1640	0.7150	0.1210	6.81	0.69
GOW-OR-11-32	14.00	45.9	0.1550	0.3520	0.4940	6.84	0.74
GOW-OR-11-33	14.50	44.9	0.1350	0.1010	0.7630	7.19	0.81
GOW-OR-11-34	9.50	49.9	0.0477	0.8190	0.1330	1.95	0.61
GOW-OR-11-35	11.80	49.9	0.0287	0.0704	0.9010	4.17	1.13
GOW-OR-11-36	13.20	51.9	0.0221	0.8490	0.1290	5.16	1.36
GOW-OR-11-37	15.00	51.9	0.0191	0.8740	0.1070	7.23	1.73
GOW-OR-11-38	11.50	50.9	0.0330	0.0706	0.8960	3.90	1.03
GOW-OR-11-39	11.70	49.9	0.0251	0.4860	0.4880	4.16	1.20
GOW-OR-11-40	14.00	51.9	0.0241	0.4390	0.5370	5.77	1.50
GOW-OR-11-41	15.00	50.9	0.0144	0.4420	0.5430	7.32	1.89
GOW-OR-11-42	9.73	49.9	0.0409	0.0872	0.8720	2.15	0.73
GOW-OR-11-43	11.30	50.9	0.0274	0.0723	0.9000	3.94	1.14
GOW-OR-11-44	14.70	50.9	0.0222	0.0855	0.8920	6.69	1.62
GOW-OR-11-45	15.30	51.9	0.0109	0.0927	0.8960	7.55	2.05

TABLE 3—C_V VALUES FOR THE TWO GEOMETRIES AND THE THREE OPENING AREAS OBTAINED FROM LINEAR REGRESSION

Choke Geometry	Orifice*	Cage
11 mm	2.55 [0.988]	2.67 [0.982]
14 mm	5.17 [1.000]	5.86 [0.997]
18 mm	8.88 [0.999]	8.73 [0.998]

*Values of correlation coefficients are shown in brackets, [r^2].

in which A = the cross-sectional area, C_T = a valve throttling coefficient (A_T/A_1), and C_C = the contraction coefficient (A_V/A_2). T and V denote throat and *vena contracta,* respectively. The mixture momentum density ρ_e is given by:

$$\frac{1}{\rho_e}=\left[\frac{x_G}{\rho_G}+k\frac{(1-x_G)}{\rho_L}\right]\left[x_G+\frac{(1-x_G)}{k}\right], \quad \ldots\ldots\ldots\ldots\ldots\ldots (18)$$

where the slip ratio is k, and x_G = the gas mass fraction.

Similarly, from cross section 2 to 3:

$$(p_3-p_B)+C_TC_X(p_B-p_2)=\frac{\dot{m}^2}{A_1^2\rho_{e1}}\left(\frac{C_X\rho_{e1}}{C_T\rho_{e2}}-C_X^2\frac{\rho_{e1}}{\rho_{e3}}\right), \quad \ldots\ldots (19)$$

where subscript B = the back wall after sudden expansion and C_X = the inlet to outlet area ratio (A_1/A_3). Because pressure recovery can be low in multiphase flows, the pressure recovery of the model can be modeled by letting C_X deviate from the actual area ratio within the range: $\frac{A_T}{A_3}\le C_TC_X\le 1$.

The total energy balance in Eq. 11 applies from Positions 1 to 2 and from 2 to 3. It is assumed that heat flux to the wall and elevation terms can be neglected for stationary flows, giving a constant stagnation enthalpy of the multiphase mixture. It simplifies the model to replace the total energy equation with a model of polytropic gas expansion. If we assume that the gas and liquid expand in thermal equilibrium without phase change (x = constant) between Positions 1 and 2, the derivation of the corresponding polytropic expansion coefficient given by Eq. 20 can be found in Henry[5] and Selmer-Olsen.[15] In Eq. 20, a small term correcting for nonhomogeneous phase velocities (slip) is neglected.

$$n=\frac{x_G\kappa C_{VG}+x_OC_{PO}+x_WC_{PW}}{x_GC_{VG}+x_OC_{VO}+x_WC_{VW}}. \quad \ldots\ldots\ldots\ldots\ldots\ldots (20)$$

Here, κ = the specific heat ratio, and C_P and C_V = the specific heats at constant pressure and volume, respectively. The subscripts G, O, and W denote gas, oil, and water, respectively. With a little liquid present, Eq. 20 will make n approach 1, and the gas will tend to expand isothermally because oil and water have the same specific heat at a constant pressure and volume.

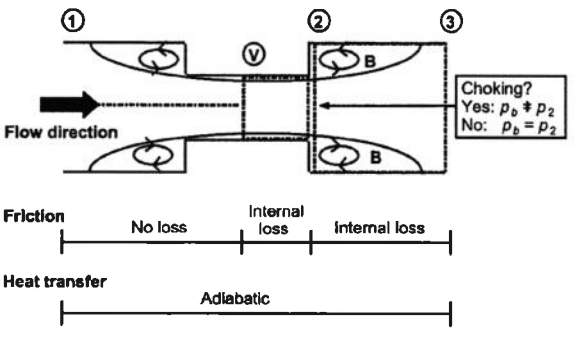

Fig. 4—Basis for the Hydro models.

TABLE 4—VALUES FOR USE WITH GROLMES AND LEUNG EQUATIONS

Model	a_0	a_1	a_2	a_3
Homogeneous (no slip)	1	1	–1	0
Constant slip	k	1	–1	0
Fauske	1	1	–1/2	0
Moody	1	1	–2/3	0
Simpson *et al.*	1	1	–5/6	0
Thom	1	1	–0.89	0.18
Baroczy	1	0.74	–0.65	0.13
Lockhart-Martenelli	0.28	0.64	–0.36	0.07

A thermodynamic software package can be used to calculate the expansion from Position 1 to Position 3 based on the assumptions that between 1 and 3, the flow is adiabatic (i.e., constant stagnation enthalpy of the multiphase mixture) and that the kinetic-energy terms of Eq. 11 can be neglected. Flashing is assumed to happen in the control volume between Positions 2 and 3 first. In this study, we used the NEW*S package.[16,17] We found that flashing and temperature change between 1 and 3 would have only a minor effect on the mixture densities, ρ_e, in 1 and 3 for the fluids and test conditions studied; hence, we simply assumed isothermal flow when calculating ρ_{e1} and ρ_{e3}.

In nonchoked (subcritical) flow, the Borda-Carnot hypothesis for sudden enlargements applies, and we can set the back wall pressure p_B=p_2. For the choked-flow case, $p_B\neq p_2$, and p_B is a free parameter that can be determined implicitly from the choked mass flow rate and the pressure, p_3. Depending on p_3, the flow is over- or under-expanded when entering the control volume at Position 2.

A criterion for choked flow is to maximize the mixture's mass flux with respect to the pressure at the choking cross section.[3] Selmer-Olsen[15] showed that this would give the same expression as the rigorous mathematical definition of critical flow as a set of three balance equations. The model gives for the critical mass flow-rate, subscript c, of the mixture.

$$\dot{m}_c^2=-\left[\frac{A^2}{\frac{d}{dp}\left(\frac{1}{\rho_e}\right)}\right]_c=-\frac{A_1^2A_T^2}{\frac{d}{dp}\left(\frac{1}{\rho_{e2}}\right)}\cdot\frac{1}{\left(\frac{1}{C_C}-1\right)^2+1}. \quad \ldots\ldots (21)$$

The critical pressure ratio, $\varepsilon_c=\frac{p_C}{p_1}$, can be found by solving the system of equations simultaneously.

Hydro Short Model. The Hydro long model described previously may be converted to what is called the Hydro short model by removing the first control volume and relocating Position V to 2, thus removing dissipation losses in the throat. The idea was that the Hydro long model should be better suited for a long-throated geometry (e.g., bean, needle, and cage chokes) and the Hydro short model for short-throated geometry (e.g., orifices and "Willis" chokes).

For short throats, the contraction of the boundary streamlines increases the flow blockage (throttling), thereby reducing the mass flow rate; however, the stagnation pressure remains constant. The contraction coefficient corrects for geometric effects only for short throats. For long throats, the contraction coefficient corrects for both geometric and loss effects. Hence, C_C has two different interpretations depending on the model. From cross section 1 to 2, Eq. 17 is replaced by:

$$\int_1^2\rho_e\frac{\rho_{e1}}{\rho_e}dp=\frac{\dot{m}^2}{2A_1^2\rho_{e1}}\left[1-\left(\frac{\rho_{e1}}{\rho_{e2}}\right)^2\frac{1}{C_T^2C_C^2}\right]. \quad \ldots\ldots\ldots\ldots (22)$$

From cross section 2 to 3, Eq. 19 is replaced by:

$$(p_3 - p_B) + C_T C_C C_X (p_B - p_2) = \frac{\dot{m}_C^2}{A_1^2 \rho_{e1}} \left(\frac{C_X}{C_T C_C} \frac{\rho_{e1}}{\rho_{e2}} - C_X^2 \frac{\rho_{e1}}{\rho_{e3}} \right). \quad \ldots\ldots\ldots\ldots\ldots\ldots\ldots\ldots (23)$$

For critical mass flow rate, Eq. 21 is replaced by:

$$\dot{m}_C^2 = -\frac{A_1^2 C_T^2 C_C^2}{\frac{d}{dp}\left(\frac{1}{\rho_{e2}}\right)}. \quad \ldots\ldots\ldots\ldots\ldots\ldots\ldots\ldots\ldots\ldots\ldots\ldots\ldots\ldots (24)$$

Slip Models for use in the Hydro Models. Flow through a choke involves strong acceleration. If the continuous phase is gas, the liquid droplets in the gas will lag behind the gas phase from the inlet position to the point of maximum velocity. Several slip models based on work in connection with flows in pipes and valves exist. For flow in chokes, however, it is not evident that the same slip models can be applied. The Chisholm slip correlation[3] given by Eq. 7 was used in the original Hydro model by Selmer-Olsen.[14]

Grolmes and Leung[6] suggested that common slip correlations could be generalized by:

$$k = a_0 \left(\frac{1 - x_G}{x_G} \right)^{(a_1 - 1)} \left(\frac{\rho_L}{\rho_G} \right)^{(a_2 + 1)} \left(\frac{\mu_L}{\mu_G} \right)^{a_3}, \quad \ldots\ldots\ldots\ldots\ldots\ldots (25)$$

in which applicable values of the constants a_0, a_1, a_2, and a_3 are given in Table 4. Dynamic viscosity is denoted by μ.

A new slip model was developed for the Hydro models based on the experimental results of this work.

$$k = \sqrt{1 + x_G \left(\frac{\rho_L}{\rho_G} - 1 \right)} \left[1 + \xi e^{-\beta x_G} \right]. \quad \ldots\ldots\ldots\ldots\ldots\ldots\ldots (26)$$

This represents an adjustment to the Chisholm expression[3] of increasing the slip, especially at low gas qualities. Based on the data in this work, suitable values for the constants were found to be $\xi = 0.6$ and $\beta = 5.0$.

The behavior of the various slip models are presented in **Fig. 5** with the slip ratio plotted as function of mass fraction of gas, x_G. The new slip model (as well as the original Chisholm expression) has the following features.

- As the gas density increases with pressure, the flow becomes more homogeneous (less slip), which is qualitatively correct because the interfacial forces increase with the gas density.
- As the gas quality, x_G, goes to zero (liquid flow only), the slip ratio, k, goes to $1+\xi \geq 1$ ($\xi = 0.6$), which is qualitatively correct because bubble flow will prevail for low qualities, with some slip still present. Fully homogeneous flow will exhibit $k = 1$.
- As the gas quality, x_G, goes to 1 (gas flow only), the slip ratio, k, goes to a value that depends on the density ratio. This is qualitatively correct for separated flows, like annular film flow, but less correct for dispersed droplet flow. For dispersed droplet flow, the slip ratio, k, should approach 1 for high gas qualities. However, in a complex flow geometry, some flow separation will always be present for high gas qualities, with some liquid attached to the wall region and some entrained in the gas phase.

Note that the effects described previously will be weighted by the balance equations for mass, momentum, and energy. It can be verified mathematically that provided the slip model gives a k value that satisfies $0 < k < \infty$ for $0 \leq x_G \leq 1$, the original Hydro model will always approach the model for pure liquid flow for $x_G = 0$ as well as the model for pure gas flow for $x_G = 1$. This means that the Hydro model becomes exactly the single-phase gas model for $x_G = 1$ and the single-phase liquid model for $x_G = 0$.

Calibration of the Hydro Models. Normally, the use of a discharge coefficient (C_D) is not required with the Hydro models; hence $C_D = 1$. The value of the contraction coefficient, C_C, is determined for single-phase water flow and also is used for multiphase flow.

In cases in which only the valve coefficient, C_V, for water flow is known from the choke manufacturer and no calibration tests can be made, a proper value for the contraction coefficient, C_C, should be selected from the literature (e.g., Weisbach values[20]). Then a value for a discharge coefficient, C_D, should be chosen by equating the mass flow rates of water given by the Hydro model and Eq. 1.

Discussion

The mass flow rate predicted by the various models was calculated based on knowledge of the upstream condition and the measured pressure drop across the choke. To compare the models, plots were made showing predicted mass flow rate vs. the measured mass flow rate.

When comparing the different models, we find that the orifice-type choke is best predicted by the Hydro short model, with $C_C = 0.62$, which corresponds to classical Weisbach values.[20] The cage-type choke with internal dissipation and losses is best predicted by the Hydro long model, with $C_C = 0.45$ based on the single-phase water experiments.

Fig. 6 shows the performance of the Hydro models using the Chisholm slip correlation. The ratio of predicted to measured mass

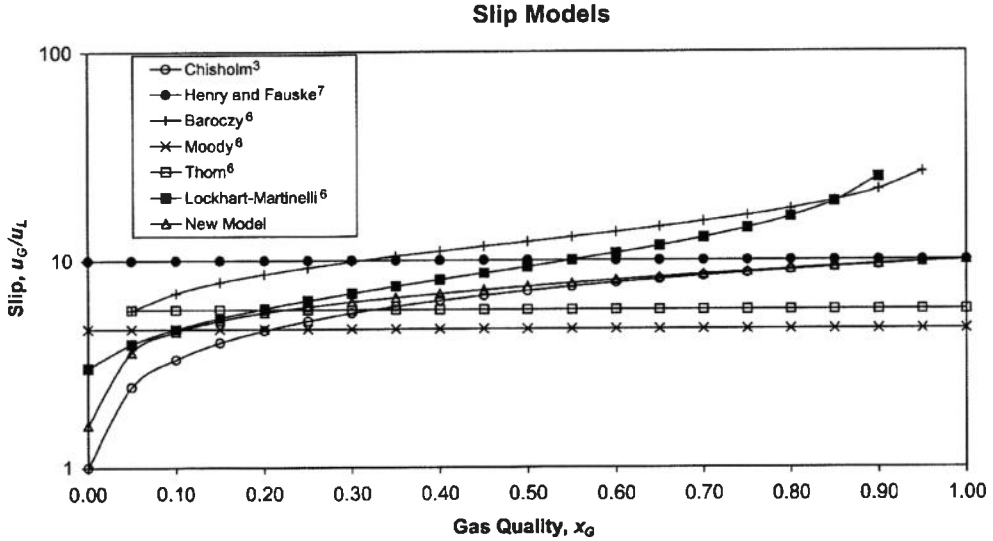

Fig. 5—Results from various slip correlations with a liquid-to-gas density ratio of 100.

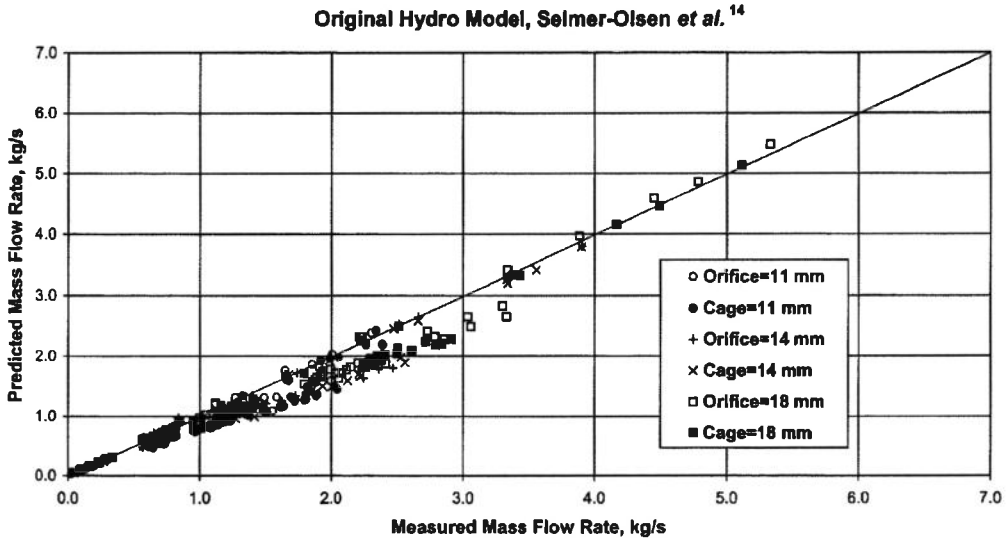

Fig. 6—Predicted vs. measured mass flow rate for the original Hydro model with Chisholm slip correlation.

flow rate, with slip predicted by the Chisholm correlation, is plotted as a function of gas quality in **Fig. 7.** It is seen that the flow rate is under-predicted, with maximum under-prediction occurring at a gas quality of approximately 0.02. Increasing the gas/liquid slip can increase the ratio. **Fig. 8** shows the improved prediction when the new slip correlation given by Eq. 26 is used.

The flow through a choke undergoes large acceleration from the upstream condition to the location of the throat. Acceleration will generally increase the slip between gas and liquid because the gas phase quickly accelerates while the liquid phase lags. Hence, acceleration will affect the system in the direction of higher slip. (The opposite is obviously the case in retarding flow downstream of the choke.)

We see from plots of different slip models that there is a large difference among their predictions. The Chisholm model often is used in calculations, but, as we have seen in this work, mass flow rates are under-predicted in the low-quality region. By modifying the slip so that it is larger than what the Chisholm correlation gives in the low-quality region, we obtain a better agreement between experimental and predicted results.

The results of the Sachdeva *et al.* model are shown in **Fig. 9,** and the results of Perkins' model appear in **Fig. 10.** Both models show a much larger spread than the Hydro models. The Sachdeva model uses a C_D of 0.85, while Perkins uses $C_D = 0.826$. Changing the value of C_D will only rotate the data set about the origin. The single-phase data are located on the line of maximum overprediction.

The results from the two-phase multiplier models give fair estimates despite compressibility effects not being included. In fact, for subcritical flow, the two-phase multiplier models give better predictions than the more physically correct models of Sachdeva *et al.* and Perkins. Both are no-slip models, but all the two-phase multiplier models have built-in slip. However, the Hydro model with the new slip correlation shown in Fig. 8 is by far the best choice. The differences between the models are given numerically in **Table 5** and graphically in **Fig. 11.** The Hydro

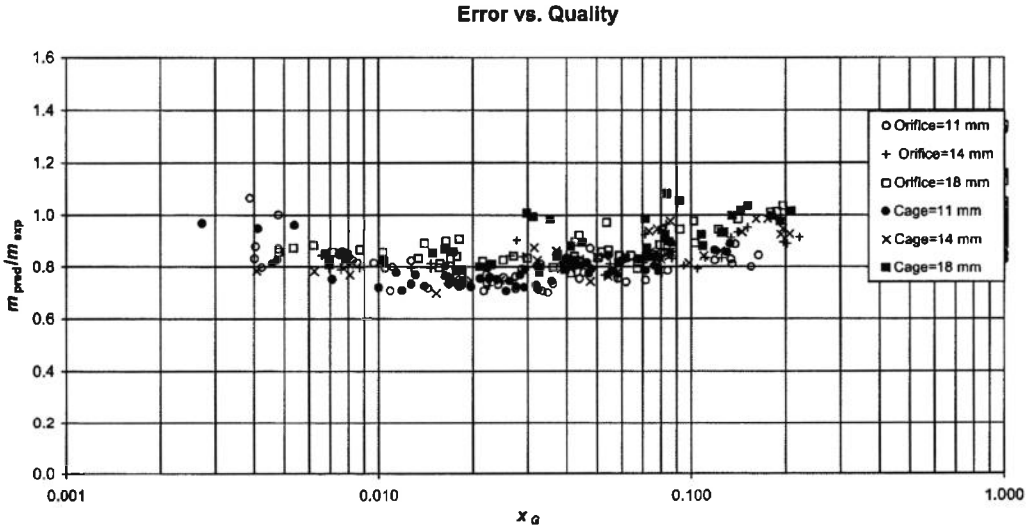

Fig. 7—Ratio of predicted to measured mass flow rate of original Hydro model as a function of gas quality with Chisholm slip correlation.

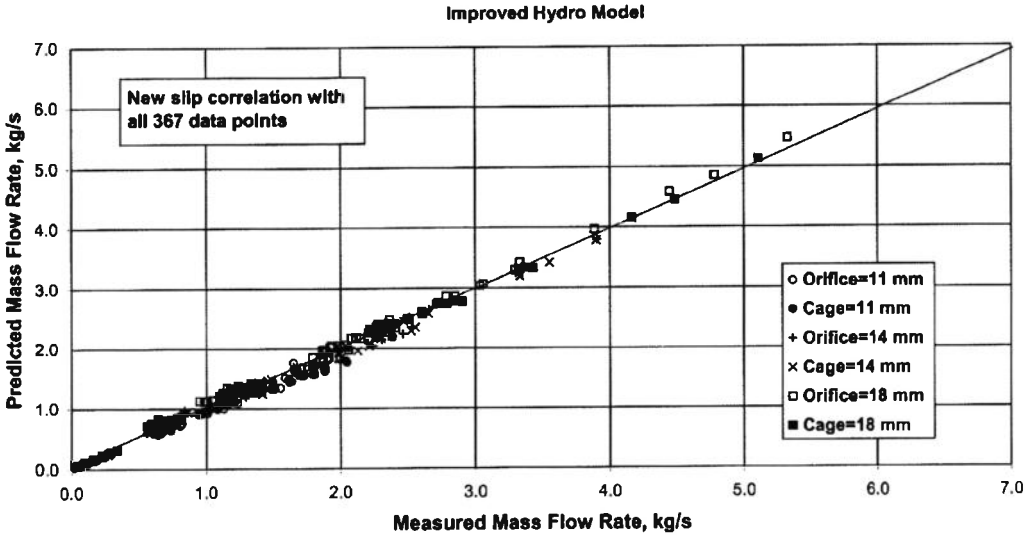

Fig. 8—Predicted vs. measured mass flow rate for all 367 tests with new slip correlation with the Hydro models.

model with the improved slip correlation gives the lowest standard deviation, 7.8%, and the lowest average error of absolute values, 5.8%. For comparison, the standard deviation for the Sachdeva *et al.* and the Perkins models are 25.8 and 32.1%, respectively. With regard to the average error of absolute values, the Sachdeva *et al.* and Perkins models exhibit values of 26.3 and 34.8%, respectively. (See Table 5 for details.) Perkins specifies standard deviations varying from 8.53 to 24.48% on his model, depending on the data set evaluated. Sachdeva *et al.* give values of standard deviation varying from 6.4 to 40.9%, depending on the data set used for evaluation.

Two choke geometries with several hole sizes were tested. The effects of choke size were not tested, but this is not expected to change the results significantly. Different choke orientation and inlet conditions were not tested and could require model calibration. Changes in fluid properties that introduce significant Reynolds-number effects or high amounts of flashing should be checked separately. The models should also be subject to evaluation for data from critical flow, including checking the transition from subcritical to critical flow.

Conclusions

A total of 367 single-, two-, and three-phase tests have been performed in the MPFL. Two different geometries, orifice and cage type, and three different opening areas (2.0, 3.5, and 5.0%) were tested. The conditions downstream of the choke were kept constant at 8 bara and 50°C. Upstream conditions were kept at a constant temperature (50°C), whereas the upstream pressures were obtained from the given volumetric flow rates.

C_V values were calculated for the different geometries and opening areas based on the single-phase water results and were used as input to the two-phase multiplier models.

Mass flow rate models are presented with the average discrepancy and standard deviation from measured values in Table 5. The Hydro models have been shown to predict the mass flow rate with the best accuracy for the new data set used in this model evaluation. $C_C = 0.62$ (based on the classical Weissbach values) is valid for orifice geometry, whereas $C_C = 0.45$ (based on single-phase water tests) gives the best value for cage geometry.

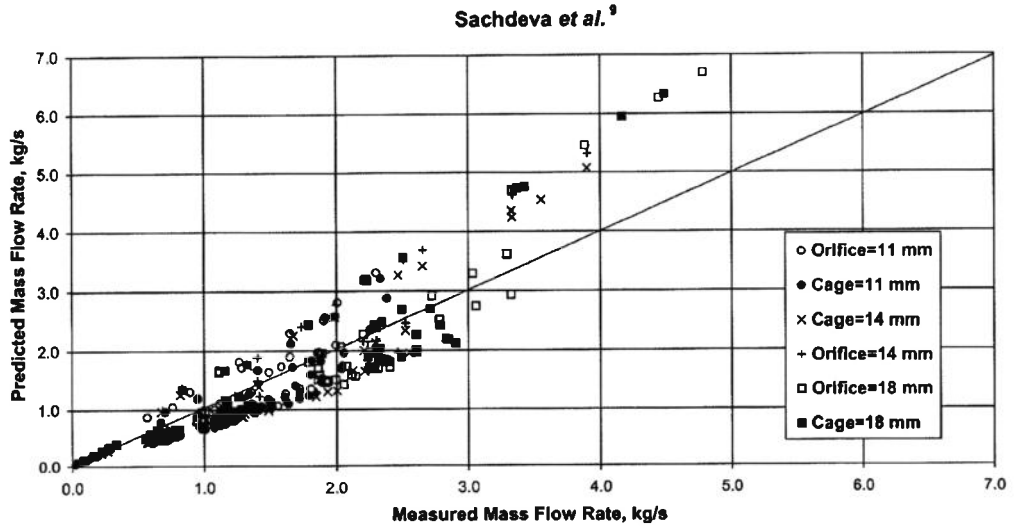

Fig. 9—Results of the Sachdeva *et al.* model.[9]

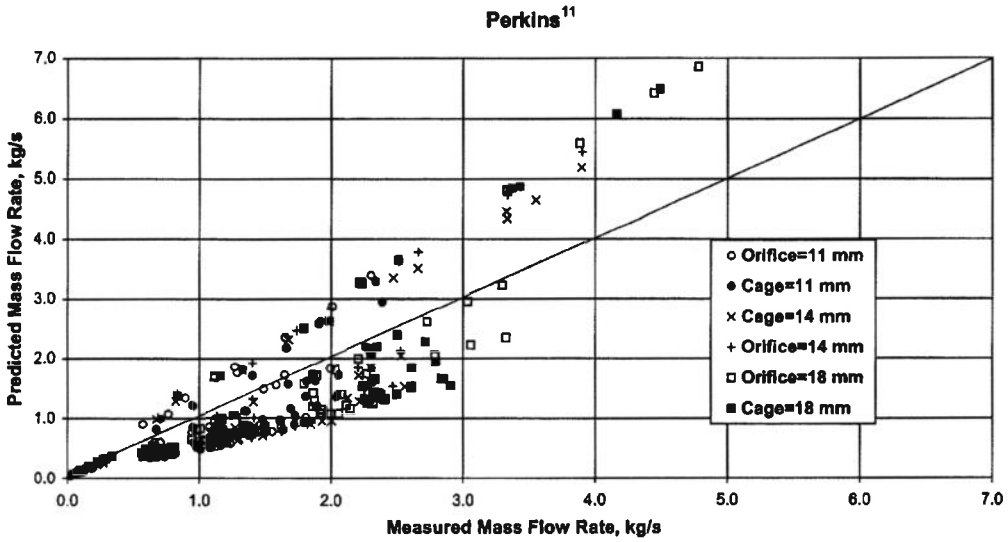

Fig. 10—Results of the Perkins model.

A new slip model that gives higher slip values for low gas qualities improves the predicted results.

The recommended model approach is the Hydro short model for orifice choke and the Hydro long model for cage-type choke.

The two-phase multiplier models give a fairly good prediction of the mass flow rates. The simplicity of these models makes them readily available as reference models. However, the Hydro models have the best overall predictive ability for subcritical flow. They also can be used for critical flow, but this has not been verified in the present work. It is recommended that these verifications are carried out.

Nomenclature

a = coefficients, dimensionless
A = area, m^2
A_C = area of *vena contracta*, m^2
B = coefficient in Morris' model, dimensionless
C_C = A_C/A_2, contraction coefficient, dimensionless
C_D = discharge coefficient, dimensionless
C_P = specific heat capacity, constant pressure, J/kg K
C_T = A_2/A_1, valve throttling coefficient, dimensionless
C_v = specific heat capacity, constant volume, J/kg K
C_V = flow coefficient for valve sizing, gal/min/psi
C_X = A_1/A_3, inlet/outlet area ratio, dimensionless
e = exponential function
F_γ = choked flow factor,[2] dimensionless
g = gravitational acceleration, m/s^2
h = enthalpy, J/kg
k = slip ratio u_G/u_L, dimensionless
$\dot{m}$ = mass flow rate, kg/s
n = polytropic gas expansion exponent, dimensionless
p = pressure, Pa
Δp = pressure difference, p_1-p_3, N/m^2
q = heat flux, W/m^2
Q = volumetric flow rate, m^3/s
T = temperature, K
u = velocity, m/s
v = specific volume $=1/\rho$, m^3/kg
W_C = water cut, dimensionless
x = mass fraction, dimensionless
z = length, dimensionless
α = A_G/A, void fraction, dimensionless
β = parameter in new slip model, dimensionless
ε_C = critical pressure ratio, p_2/p_1, dimensionless
θ = angle of flow path, radians
κ = ratio of specific heats, C_P/C_v, dimensionless
μ = dynamic viscosity, kg/m s
ξ = parameter in new slip model, dimensionless
ρ = density $=1/v$, kg/m^3
τ_w = wall shear stress, Pa
ϕ_w = wall perimeter, m
Φ = two phase multiplier $\Delta p/\Delta p_{LO}$, dimensionless

TABLE 5—MODEL COMPARISON WITH ALL 367 DATA POINTS

Model	Average Error (%)	Standard Deviation (%)	Average Error of Absolute Values (%)
Hydro models with new slip model	–0.36	7.76	5.78
Hydro models with Chisholm slip model	–12.43	10.51	13.92
Sachdeva *et al.*	–6.07	25.77	26.25
Perkins	–19.78	32.13	34.82
Homogeneous Equilibrium Model – Φ^2_{LO}	–20.82	15.94	23.11
Simpson *et al.* – Φ^2_{LO}	–8.68	11.59	11.29
Chisholm – Φ^2_{LO}	–11.05	13.48	13.52
Morris – Φ^2_{LO}	–16.34	13.36	18.09

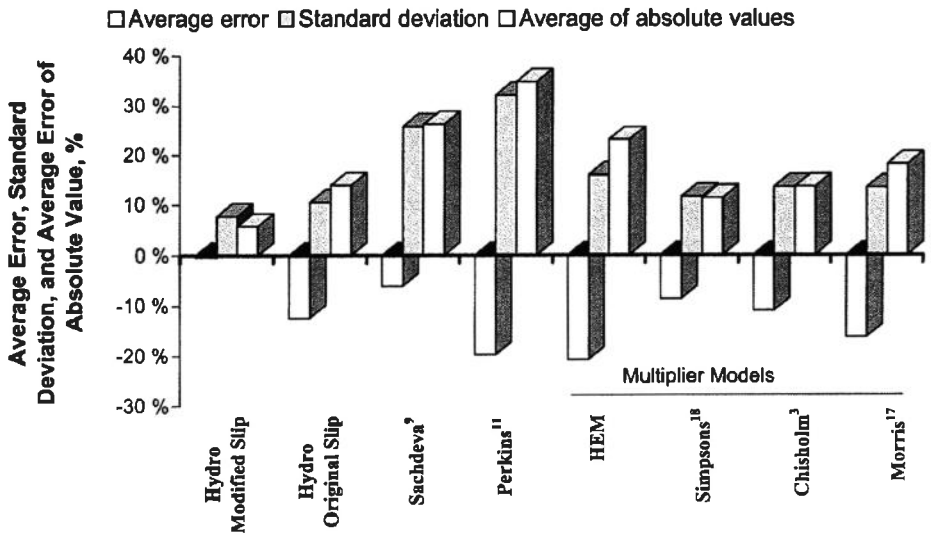

Fig. 11—Prediction accuracy and standard deviation of the different mass-flow-rate models.

Subscripts

B = back wall of sudden enlargement
c = choked
e = momentum density
exp = experimental results
G = gas
H = homogeneous mixture
k = kinetic energy
L = liquid
LO = liquid only
m = mixture
O = oil
pred = model prediction
T = position at vena contracta
W = water
1 = position upstream choke
2 = position in the throat (at throat exit)
3 = position downstream choke (at "recovered conditions")

Acknowledgments

The results reported in this paper are part of a cooperative project between Norsk Hydro, Statoil, and TotalFinaElf. The authors are indebted to the technicians at the Multiphase Flow Loop.

References

1. Robertson, D.S., Morgan, G.E., and Lang, I.W.P.: "Flashing flow through wellhead chokes: An experimental study," Third Intl. Conference on Multiphase Flow, BHRA, The Hague (1987).
2. Driskell, L.: *Control-Valve Selection and Sizing*, The Instrument Society of America, Research Triangle Park, North Carolina (1983).
3. Chisholm, D.: *Two-Phase Flow in Pipelines and Heat Exchangers*, George Godwin (Longman Group Ltd.) and IChemE, London (1983).
4. Tangren, R.F., Dodge, C.H., and Seifert, H.S.: "Compressibility effects in two-phase flow," *J. Applied Physics* (1949) **20**, No. 7, 637.
5. Henry, R.E.: "Two-Phase Flow Dynamics," *Hemisphere* (1981).
6. Grolmes, M.A. and Leung, J.C.: *Chemical Engineering Progress* (1985) **81**, No. 8, 47.
7. Henry, R.E. and Fauske, H.K.: "The two-phase critical flow of two-component mixtures in nozzles, orifices and short tubes," *TASME J. Heat Transfer* (1971) **93**, No. 2, 179.
8. *RP 521, Guide for Pressure Relief and Depressuring Systems*, API, Washington, D.C. (1990).
9. Sachdeva, R. *et al.*: "Two-Phase Flow Through Chokes," paper SPE 15657 presented at the 1986 SPE Annual Technical Conference and Exhibition, New Orleans, 5–8 October.
10. Singleton, E.W.: "Development of a high-performance choke valve with reference to sizing for multiphase flow," *Measurement and Control* (1991) **24**, 273.
11. Perkins, T.K.: "Critical and Sub-critical Flow of Multiphase Mixtures Through Chokes," *SPEDC* (December 1993) 271.
12. Osman, M.E. and Dokla, M.E.: "Correlations predict gas-condensate flow through chokes," *Oil & Gas J.* (1992) **90**, No. 11, 43.
13. Selmer-Olsen, S.: "Subsea Choke Flow Characteristics," DNV Research Report No. 92-2054, Det Norske Veritas, Norway (1992).
14. Selmer-Olsen, S. *et al.*: "Subsea Chokes as Multiphase Flowmeters. Production Control at Troll Olje," paper presented at the 7th Intl. Conference on Multiphase Production, BHR Group, Cannes, France (1995) 441.
15. Selmer-Olsen, S.: "Etude théorique et expérimentale des écoulements diphasiques en tuyére convergente-divergente," PhD dissertation, l'Inst. Natl. Polytechnique de Grenoble (INPG), Grenoble, France (1991).
16. Wilson, A. *et al.*: "Creating, Implementing and Verifying an Engineering Tool," paper presented at the 1991 Gas Processors Assoc. Annual Convention. San Antonio, Texas, March.
17. Overå, S.: *NEW*S—A New Process Simulator*, NPF, Norwegian Petrochemical Society (1989).
18. Morris, S.D.: "Two-Phase Pressure Drop Across Valves and Orifice Plates in European Two-Phase Flow Group Meeting," paper E2, Marchwood Engineering Laboratories, Southhampton, U.K. (1985) 4–7 June.
19. Simpson, H.C., Rooney, D.H., and Grattan, E.: "Two-phase flow through gate valves and orifice plates," paper presented at the 1983 Intl. Conference on the Physical Modelling of Multiphase Flow, Coventry, England, 19–21 April.
20. Hewitt, G. and Hall-Taylor, N.S.: *Annular Two-Phase Flow*, Pergamon Press, Oxford, England (1970).

SI Metric Conversion Factors

bar × 1.0*	E+05 =	Pa
°F (°F−32)/1.8	=	°C
gal × 3.785 412	E−03 =	m^3
psi × 6.894 757	E+00 =	kPa

*Conversion factor is exact.

Reidar Barfod Schüller is currently an associate professor with the Agricultural U. of Norway. e-mail: reidar.schuller@inf.nlh.no. He has worked with the Research Division of Det Norske Veritas and also has industrial research experience from Norsk Hydro ASA, especially in experimental multiphase flow with special focus on real hydrocarbon/watersystems. Schüller holds a PhD degree in mechanical engineering from Heriot-Watt U., Edinburgh, U.K. **Trond Solbakken** is currently an adviser in Fluid Mechanics & Multi-Phase Flow with Norsk Hydro ASA, Sector for Operation & Production. e-mail: Trond.Solbakken@hydro.com. He has worked with CFD-modeling and experiments on two-phase flow at the research institute, Tel-Tek/HiT, and later with industrial flow studies on multiphase hydrocarbon systems at Norsk Hydros multiphase lab in Porsgrunn. Solbakken holds an MS degree in process engineering from Telemark U. College (HiT), Porsgrunn, Norway. **Staale Selmer-Olsen** is currently the Research Program Director in DNV Research, which is the corporate research and development unit of Det Norske Veritas AS. e-mail: Staale.Selmer-Olsen@dnv.com. He has industrial and applied research experience from both modeling and experimental work with multiphase flow in hydrocarbon, chemical, and other industries. Selmer-Olsen holds a PhD degree in mechanical engineering that addressed critical and noncritical multiphase flow through flow restrictions from I.N.P.G. in Grenoble, France. He also holds a post-graduate diploma from the von Karman Inst. for Fluid Dynamics, Belgium, and an MS degree in mechanical engineering from the Norwegian Inst. of Technology, Trondheim, Norway.